J. Biochem. **139**, 931–939 (2006)
doi:10.1093/jb/mvj105

CIN85 Is Localized at Synapses and Forms a Complex with S-SCAM *via* Dendrin

Akira Kawata, Junko Iida, Mitsunobu Ikeda, Yuji Sato, Hiroki Mori, Ai Kansaku, Kazutaka Sumita, Naoyuki Fujiwara, Chiaki Rokukawa, Mamiko Hamano, Susumu Hirabayashi and Yutaka Hata*

Department of Medical Biochemistry, Graduate School of Medicine, Tokyo Medical and Dental University, Tokyo 113-8519

Received March 21, 2006; accepted April 13, 2006

Membrane-associated guanylate kinase inverted (MAGI)-1 plays a role as a scaffold at cell junctions in non-neuronal cells, while S-SCAM, its neuronal isoform, is involved in the organization of synapses. A search for MAGI-1–interacting proteins by yeast two-hybrid screening of a kidney cDNA library yielded dendrin. As dendrin was originally reported as a brain-specific postsynaptic protein, we tested the interaction between dendrin and S-SCAM and revealed that dendrin binds to the WW domains of S-SCAM. Dendrin is known to be dendritically translated but its function is largely unknown. To gain insights into the physiological meaning of the interaction, we performed a second yeast two-hybrid screening using dendrin as a bait. We identified CIN85, an endocytic scaffold protein, as a putative dendrin-interactor. Immunocytochemistry and subcellular fractionation analysis supported the synaptic localization of CIN85. The first SH3 domain and the C-terminal region of CIN85 bind to the proline-rich region and the N-terminal region of dendrin, respectively. *In vitro* experiments suggest that dendrin forms a ternary complex with CIN85 and S-SCAM and that this complex formation facilitates the recruitment of dendrin and S-SCAM to vesicle-like structures where CIN85 is accumulated.

Key words: dendrites, endocytosis, scaffold, synapses.

Membrane-associated guanylate kinase inverted (MAGI) family is composed of three members, MAGI-1, S-SCAM (also called as MAGI-2) and MAGI-3. MAGI-1 is localized at tight junctions in polarized epithelial cells and at the slit diaphragm in kidney podocytes (*1–3*). MAGI-1 is attached to membrane proteins such as junctional cell adhesion molecule 4, nephrin, megalin, endothelial adhesion molecule and muscle-specific receptor tyrosine kinase (*3–7*). It interacts with cytoskeleton adaptor proteins (α-actinin-4, synaptopodin, Carom and β-catenin) and regulators for small GTP-binding proteins (RapGEP, neuroepithelial cell transforming gene 1 and PDZ-GEF1) (*8–13*). MAGI-3 is also expressed in various tissues. The list of reported MAGI-3-ligands includes Frizzled, Ltap, phosphatase and tensin homolog (PTEN), receptor tyrosine phosphatase beta and transforming growth factor alpha (TGFα) precursor (*14–17*). The message of S-SCAM is detected only in brain and is regarded as a neuronal member of MAGI family proteins (*18*). Like MAGI-1 and MAGI-3, S-SCAM binds various proteins (*N*-methyl-D-aspartate receptor subunits, δ2 glutamate receptor, activin type II receptor, β1-adrenergic receptor, neuroligin, Dasm1, TGFα precursor, β-catenin, δ-catenin, PTEN, PDZ-GEF1 and atrophin-1) and plays a role in the assembly of synaptic components (*17–27*). S-SCAM binds other scaffold proteins such as PSD-95, Axin and MAGUIN/Cnk2 (*28–30*). These interactions suggest that MAGI family proteins are positioned as hubs in a large protein network at tight junctions, the slit diaphragm and synapses. Therefore, the study of yet unidentified protein–protein interactions that MAGI family proteins mediate will help our understanding of how cell junctions are organized and regulated.

We searched for MAGI-1–interacing proteins by a yeast two-hybrid screening and encountered dendrin. Dendrin was originally identified as a rat brain protein. In the first paper, the transcript was reported as brain-specific (*31*). The second paper described that it is almost exclusively detected in forebrain structures (*32*). Its mRNA and the protein associated with polyribosomes are detected in dendrites, suggesting that the protein is dendritically translated. These findings prompted researchers to speculate that dendrin is implicated in cytoskeletal modulation of dendrites and synaptic plasticity. However, substantial evidence to support this idea is currently missing. We obtained dendrin from a kidney cDNA library. We confirmed the expression of this protein in kidney using a specific antibody, but consistent with the preceding reports, the expression was higher in brain than in kidney. Since the molecular organization is well conserved among MAGI family proteins and they share the same proteins as ligands, we characterized the binding of dendrin to S-SCAM. Moreover, to gain insights into the significance of this interaction, we performed a second yeast two-hybrid screening using dendrin as a bait. We identified CIN85 as a putative interactor for dendrin. CIN85 is well studied, and accumulating evidence supports that it functions as a scaffold protein in endocytosis and apoptosis (*33*). We report here that dendrin may link two scaffold proteins, S-SCAM

*To whom correspondence should be addressed. Tel: +81-3-5803-5164, Fax: +81-3-5803-0121, E-mail: yuhammch@med.tmd.ac.jp

and CIN85, and contribute to the formation of protein–protein interaction webs at dendritic spines.

MATERIALS AND METHODS

Construction of Expression Vectors—Human cDNAs of dendrin and CIN85 were obtained by PCR using primers (5′-gaattcctggatggcccactgttctc-3′ and 5′-gcggccgcctctcactgcctcttcct-3′ for dendrin; 5′-gaattcgtggaggccatagtggagtt-3′ and 5′-gtcgactattttgattgtagagctttc-3′ for CIN85) on human brain cDNA (BioChain Institute Inc.). pET32a vector was purchased from Takara Biotechnology. pClneo-Myc, pBudCE2 and pBTM116KM vectors were described previously (*3*, *18*, *34*). pClneoFLAG vector was generated by ligating linkers (5′-ctagccggggccatggactacaaagacgatgacgacaagg-3′ and 5′-aattccttgtcgtcatcgtctttgtagtccatggccccgg-3′) into *Nhe*I/*Eco*RI sites of pClneo vector (Promega). The following dendrin and CIN85 constructs encode the indicated amino acids of human dendrin and CIN85; pClneo-Myc, pClneoFLAG and pBTM116KM dendrin-1, 2-711; pClneoMyc, pClneoFLAG and pBTM116KM dendrin-2, 136-711; pClneoMyc, pClneoFLAG and pBTM116KM dendrin-3, 381-711; pClneoMyc, pClneoFLAG and pBTM116KM dendrin-4, 2-381; pClneoMyc, pClneoFLAG dendrin-5, 136-381; pClneoMyc, pClneoFLAG dendrin-6, 2-143; pClneoMyc, pClneoFLAG and pET32a CIN85-1, 2-685; pGex4T-1 CIN85-2, 2-79; pGex4T-1 CIN85-3, 66-236; pGex4T-1 CIN85-4, 219-393; and pGex4T-1 CIN85-5, 348-685. pBudCE-FLAG-CIN85-1-GFP-dendrin-1 vector was prepared from pBudCE2 vector and harbors FLAG-CIN85-1 under cytomegalovirus immediate-early promoter and GFP-dendrin-1 under elongation factor 1α-subunit promoter. PCR was performed using primers (5′-gaattcagcgcccatagtggctcc-3′ and 5′-gtcgactctcactctctctttccc-3′) on rat brain cDNA to generate pGex4T-1 dendrin-C encoding the C-terminal 64 amino acids of rat dendrin. pClneoMyc S-SCAM-1, -3, pMal S-SCAM-N, -M and -C were described previously (*18*, *29*). S-SCAM and MAGI-1 constructs encode the indicated amino acids of rat S-SCAM and MAGI-1; pGex4T-1 S-SCAM-24, 1-302; pGex4T-1 S-SCAM-WW, 303-405; pGex4T-1 S-SCAM-WW1, 303-344; pGex4T-1 S-SCAM-WW2,. 340-395; pBTM116KM MAGI-1–8, 430-1256. Constructs used in this study were summarized (Fig. 1).

Antibodies and Reagents—Rabbit antibody against WW domains of S-SCAM was described previously (*18*). Rabbit anti-dendrin and anti-CIN85 antibodies were raised against the products of pGex4T-1 dendrin-C and pET32a-CIN85. Because the C-terminal sequences of rat dendrin and human dendrin differ, we used rat dendrin as an immunogen, but the antibody recognizes human dendrin, too. The following antibodies and reagents were purchased from commercial sources: mouse monoclonal anti-Myc 9E10 (American Type Culture Collection); mouse monoclonal anti-FLAG, rabbit polyclonal anti-FLAG and Hoechst 33342 (Sigma-Aldrich); mouse monoclonal anti-synaptophysin (Roche Molecular Biochemicals); mouse monoclonal anti-EEA1 and mouse monoclonal anti-Lamp1 (BD Biosciences Pharmingen); tetramethylrhodamine-conjugated epidermal growth factor (EGF) (Molecular Probes); and secondary antibodies for dual labeling (Chemicon International Inc.).

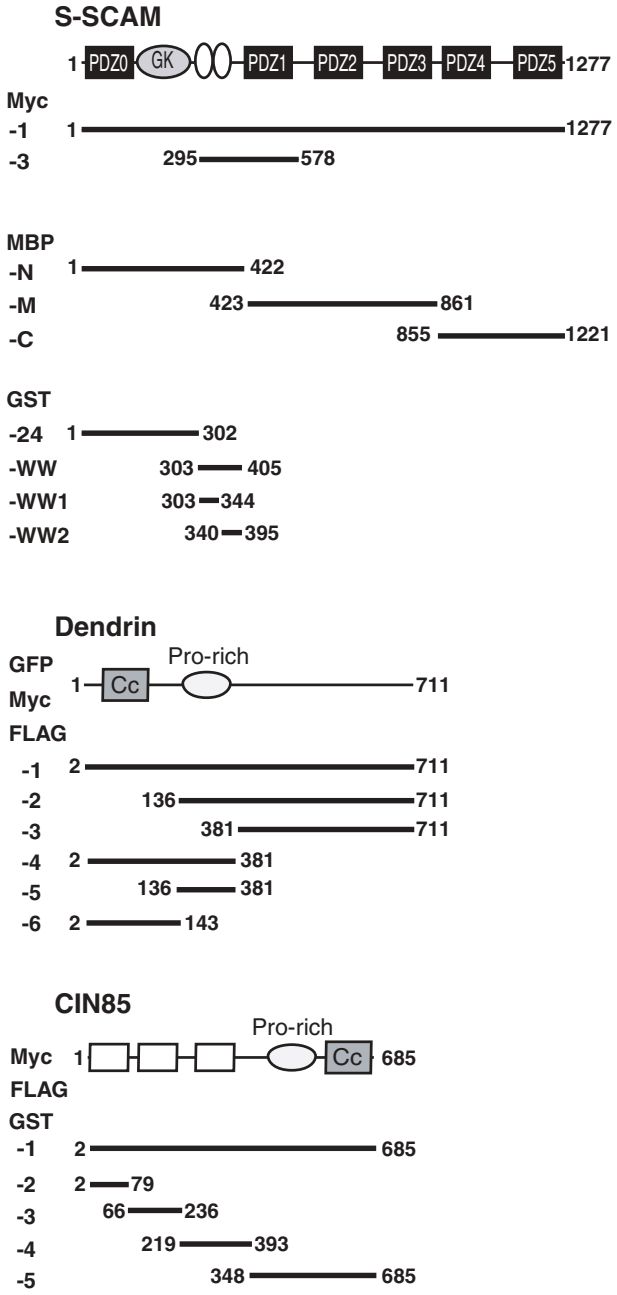

Fig. 1. **Schematic drawing of S-SCAM, dendrin and CIN85 constructs used in this study.** S-SCAM, dendrin and CIN85 proteins were expressed as Myc-tagged, FLAG-tagged, glutathione S-transferase (GST)-fusion and maltose-binding protein (MBP)-fusion proteins. Black boxes, gray oval and white ovals show PDZ, guanylate kinase (GK) and WW domains in S-SCAM. Gray boxes and white ovals represent coiled-coil (Cc) domains and proline-rich (Pro-rich) regions in dendrin and CIN85. SH3 domains are depicted as white boxes in CIN85. Numbers indicate those of the first and the last amino acid residues of each protein.

Yeast Two-Hybrid Screening—Yeast two-hybrid screening was performed using human kidney and brain cDNA libraries (Clontech Laboratories Inc.) and yeast strain L40. Histidine selection plates contained 8 mM

3-amino-1,2,4-triazole and 360 mg/liter of 5-bromo-4-chloro-3-indolyl-β-D-galactopyranoside. After 6 days of incubation, blue colonies were picked up for further analysis.

Cell Culture and Protein Expression—All procedures related to the care and treatment of animals were in accordance with institutional guidelines. Hippocampal neuron cultures were performed from E18 embryos as described previously (*18*). COS-7 cells were grown in cultures in Dulbecco's modified Eagle medium supplemented with 10% fetal bovine serum, 100 U of penicillin/ml, and 100 μg of streptomycin/ml under 5% CO_2 at 37°C. COS-7 cells were transfected by the DEAE-dextran method.

Immunocytochemistry—Hippocampal neurons were fixed with PBS containing 4% (w/v) paraformaldehyde and 4% (w/v) sucrose for 15 min, or cold methanol for 10 min at –20°C, and permeabilized with 0.25% (w/v) Triton X-100 in PBS for 5 min. After being blocked with PBS containing 10% (w/v) BSA, cells were incubated with the first antibody in PBS containing 3% (w/v) BSA overnight, washed with PBS and incubated with the second antibody in PBS containing 3% (w/v) BSA for 2 h. After a wash with PBS, the samples were embedded in 95% (w/v) glycerol in PBS. COS-7 cells were fixed with 4% (w/v) formaldehyde in PBS at 37°C for 15 min, blocked with 50 mM glycine in PBS for 30 min, and incubated subsequently with 0.2% (w/v) Triton X-100 in PBS for 15 min and with 1% (w/v) BSA in PBS for 30 min at room temperature. Cells were incubated with the first antibodies in PBS containing 1% (w/v) BSA and 0.1% (w/v) Triton X-100 for 4 h at 4°C, washed with 0.1% (w/v) Triton X-100 in PBS three times, incubated with the second antibodies in PBS containing 1% (w/v) BSA and 0.1% (w/v) Triton X-100 for 4 h at room temperature. After a wash with PBS containing 0.1% (w/v) Triton X-100, the samples were embedded in 95% (w/v) glycerol in PBS. For EGF incorporation assay, COS-7 cells were incubated at 4°C for 1.5 h in Dulbecco's modified Eagle medium containing 500 ng/ml of tetramethylrhodamine-conjugated EGF and 0.05% (w/v) BSA, washed with ice-cold PBS, and incubated at 37°C for 30 min, 3 h or 6 h. Images were obtained by use of an Olympus IX71 CCD microscope with 40× objective.

Immunoprecipitation—COS-7 cells were co-transfected by use of DEAE-dextran with various tagged constructs. Cells from each 10-cm diameter plate were homogenized in 300 μl of 50 mM Tris-HCl (pH 8.0), 100 mM NaCl, 1% (w/v) deoxycholic acid, 1% (w/v) Triton X-100 and centrifuged at 100,000 × *g* for 15 min at 4°C. The supernatant was diluted with an equal volume of 25 mM Tris-HCl (pH 8.0) containing 100 mM NaCl, then incubated with preimmune serum or anti-dendrin antibody fixed on 5 μl of protein G Sepharose 4 fast-flow beads. For immunoprecipitation of endogenous proteins, two rat brains were gently homogenized in 16 ml of 4 mM Hepes-NaOH at pH 7.4 containing 0.32 M sucrose and centrifuged at 800 × *g* for 10 min at 4°C. The supernatant was centrifuged at 9,200 × *g* for 15 min at 4°C. The resulting pellet was resuspended in 4 ml of 20 mM Hepes-NaOH (pH 8.0) containing 100 mM NaCl, 1% (w/v) deoxycholic acid and 1% (w/v) Triton X-100 and centrifuged at 100,000 × *g* for 30 min at 4°C. The supernatant was diluted with an equal volume of 20 mM Hepes-NaOH (pH 8.0) containing 100 mM NaCl and incubated with either preimmune or anti-dendrin antibody fixed on 5 μl of protein G Sepharose 4 fast-flow beads. The beads were washed four times with 20 mM Hepes-NaOH (pH 8.0) containing 100 mM NaCl and 1% (w/v) Triton X-100, and then proteins on the beads were analyzed by SDS-PAGE and immunoblotted with various antibodies.

Pull-Down Assay—COS-7 cells were transfected by the DEAE-dextran method with various tagged constructs. Cells from one 10-cm plate were homogenized in 300 μl of 50 mM Tris-HCl (pH 8.0), 100 mM NaCl, 1% (w/v) deoxycholic acid and 1% (w/v) Triton X-100, and then centrifuged at 100,000 × *g* for 15 min at 4°C. For each extract, 200 μl was incubated with 250 pmol of various glutathione S-transferase (GST)– or maltose-binding protein (MBP)–fused proteins fixed on 10 μl of glutathione Sepharose beads or amylose resins. For GST-CIN85-2 and -5, 500 pmol of each construct was used. After the beads had been washed, the proteins on the beads were immunoblotted with various antibodies.

RESULTS

Identification of Dendrin as a Binding Partner for MAGI Proteins and Its Expression in Non-Neuronal Tissues—MAGI-1 interacts with various components of epithelial cell junctions and is involved in the organization of cell junctions. To further clarify the role of MAGI-1 as a scaffold in epithelial cells, we performed a yeast two-hybrid screening on a human kidney cDNA library using the C-terminal region of MAGI-1 encompassing four PDZ domains as a bait. We obtained 24 positive clones, one of which encoded the C-terminal 289 amino acids of human dendrin. Originally, dendrin was identified as a brain protein and its expression in kidney was not characterized (*31*, *32*). We therefore raised an antibody and examined the tissue distribution of dendrin. The antibody recognized two bands in brain as previously reported (Fig. 2). Signals were also detected in other tissues including spleen, liver, kidney and placenta. This result indicates that dendrin is not brain-specific. However, as the expression of dendrin in kidney is lower than in brain, and MAGI family proteins share the same proteins, for instance β-catenin, PTEN, PDZ-GEF1 and TGFα precursor, we speculated that S-SCAM may be a neuronal binding-partner for dendrin (*10,11,15,17,23,25,26*,). To test this assumption, we immunoprecipitated dendrin from brain. The upper band detected by anti-dendrin antibody was overlapped by IgG that remained as an oligomer even after

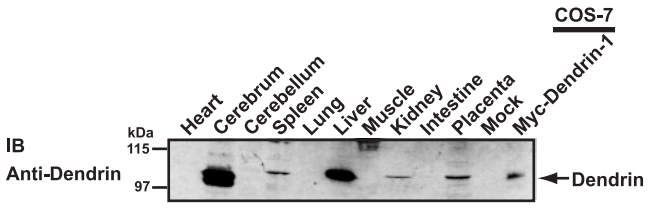

Fig. 2. **Tissue distributions of dendrin.** Immunoblotting of various rat tissue lysates. Lysates (15 μg of total protein per lane) were immunoblotted with anti-dendrin antibody. COS-7 cells transfected with mock or pClneoMyc dendrin-1 were run as negative and positive controls. Protein standards are indicated on the left in kilodaltons.

2-mercaptoethanol treatment (Fig. 3A, upper panel, asterisks and arrows). However, close observation revealed that the anti-dendrin antibody indeed immunoprecipitated endogenous dendrin. The lower band of dendrin was more clearly detected in the immunoprecipitate (Fig. 3A, arrowheads). We immunoblotted the immunoprecipitate by anti–S-SCAM antibody and detected S-SCAM in it (Fig. 3A, lower panel). Next, we examined which region of S-SCAM interacts with dendrin. Although we obtained dendrin using the C-terminal region of MAGI-1 in the yeast two-hybrid screening, dendrin bound to the N-terminal region of S-SCAM in the pull-down assay using heterologous cells (Fig. 3B, top panel). Additional experiments revealed that both of WW domains of S-SCAM are capable of binding dendrin (Fig. 3B, middle and bottom panels). To determine the S-SCAM–interacting region, we performed a pull-down assay using GST-S-SCAM-WW and various Myc-tag constructs of dendrin. Among tested proteins, Myc-dendrin-2, -4 and -5 were captured by GST-S-SCAM-WW, while neither Myc-dendrin-3 nor -6 was (Fig. 3C). PPXY is a minimum consensus motif for the major group of WW domain (*35*). Because Myc-dendrin-5 harbors two PPSY and one PPPY, it is likely that these sequences are responsible for the interaction with S-SCAM. To resolve the discrepancy between the results from the yeast two-hybrid screening for MAGI-1 and the pull-down assays for S-SCAM, we also performed *in vitro* interaction assays using various MAGI-1 constructs. In the pull-down assays, dendrin interacted with the WW domains of MAGI-1, but not with the C-terminal region (data not shown). Although we can not completely exclude the possibility that dendrin also binds to a different region of S-SCAM with a lower affinity, the *in vitro* experiments indicate that the WW domains of S-SCAM are major interacting sites for dendrin.

Identification of CIN85 as a Binding Partner for Dendrin and Its Synaptic Localization—Dendrin is speculated to modulate the structure of dendrites based on the translation of its dendritically localized mRNA. However, substantial evidence for this idea is currently missing. To elucidate how dendrin functions in brain, we performed a second yeast two-hybrid screening on a human brain cDNA library using the full-length, the N-terminal and the C-terminal dendrin constructs as baits. In this screening, we obtained one clone encoding the C-terminal 587 amino acids of human CIN85 (also called SETA and Ruk) (*33*, *36–38*). CIN85 is a multi-adaptor protein with three SH3 domains, a proline-rich region and a C-terminal coiled-coil domain. Its expression in brain has been reported, but its subcellular localization in neurons is not yet known. We immunoblotted rat brain subcellular fractions with anti-CIN85 antibody. Both CIN85 and dendrin were detected in various fractions including the postsynaptic density fraction (Fig. 4A). In the immunocytochemistry, CIN85 showed a somatodendritic distribution, but also formed clusters apposed to synaptophysin clusters at synapses (Fig. 4B, arrows). As all antibodies against S-SCAM, dendrin and CIN85 are rabbit antibodies, and anti-dendrin antibody is not suitable for immunocytochemistry, we did not directly compare the localizations of these proteins in double immunocytostaining. However, the co-localization of CIN85 and synaptophysin supports the notion that CIN85 is localized at synapses. To confirm

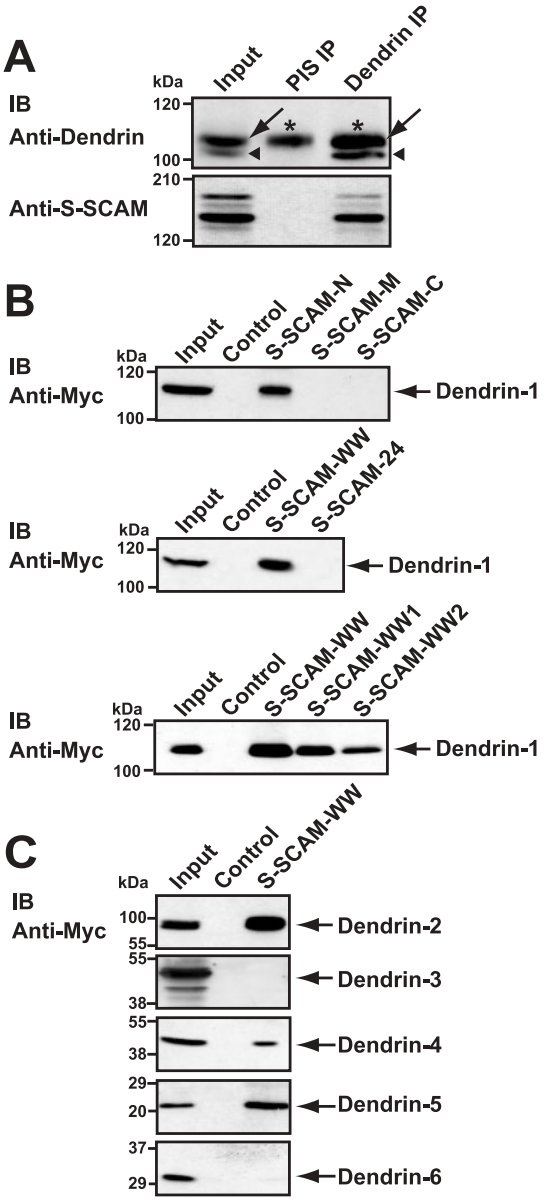

Fig. 3. **Interaction between S-SCAM and dendrin.** (A) Co-immunoprecipitation of dendrin and S-SCAM *in vivo*. Rat brain lysates were incubated with either the pre-immune or anti-dendrin antibody immobilized on protein G Sepharose beads. After the beads had been washed, the precipitates were analyzed by SDS-PAGE and immunoblotted with anti-dendrin and anti–S-SCAM antibodies. The lysate (20 μg of total protein) used for immunoprecipitation was run as input control (Input). Anti-dendrin antibody detected two bands (arrows and arrowheads). Asterisks correspond to IgG that remained as an oligomer even after 2-mercaptoethanol treatment. Protein standards are indicated on the left. (B) Mapping of dendrin-interacting region of S-SCAM. Pull-down assays were performed using lysates of COS-7 cells expressing Myc-dendrin-1 with various MBP proteins immobilized on amylose resin (top panel) or GST proteins immobilized on glutathione-Sepharose beads (middle and bottom panels). MBP-S-SCAM-N, GST-S-SCAM-WW, WW1 and WW2 trapped Myc-dendrin-1. (C) Mapping of S-SCAM–interacting region of dendrin. Pull-down assays were performed using lysates of COS-7 cells expressing various Myc-tagged dendrin proteins with GST-S-SCAM-WW immobilized on glutathione-Sepharose beads. Dendrin-2, -4 and -5 were captured by GST-S-SCAM-WW.

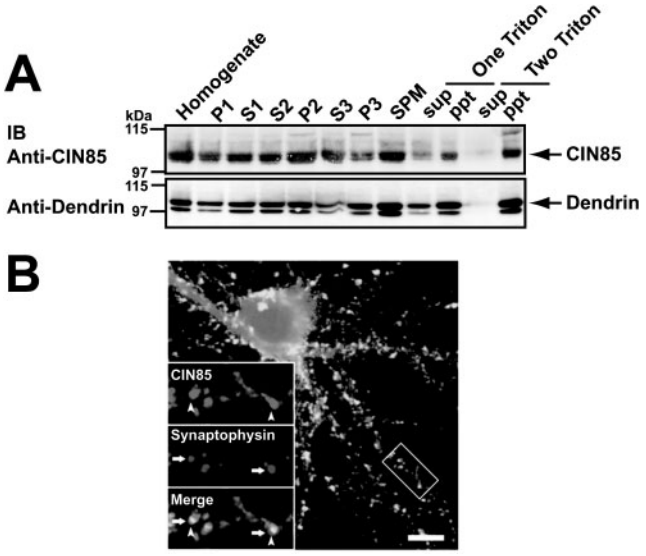

Fig. 4. **Subcellular localization of CIN85 in neurons.** (A) CIN85 and dendrin in the subcellular fractions of rat brain. P1, the nuclear pellet; S1, the crude synaptosomes; S2, the cytosol of synaptosomes; P2, crude synaptosomal pellets; S3, crude synaptic vesicles; P3, lysed synaptosomal membranes; and SPM, synaptic plasma membranes. SPM fraction was extracted with 0.5% (w/v) Triton X-100 (One Triton) and subsequently with 1.0% (w/v) Triton X-100 (Two Triton). Each lane contains 15 μg of total protein. Protein standards are indicated on the left. (B) Immunofluorescence of endogenous CIN85 and synaptophysin in rat hippocampal neurons. Rat hippocampal neurons were immunostained with rabbit anti-CIN85 and mouse anti-synaptophysin antibodies. Bar, 10 μm.

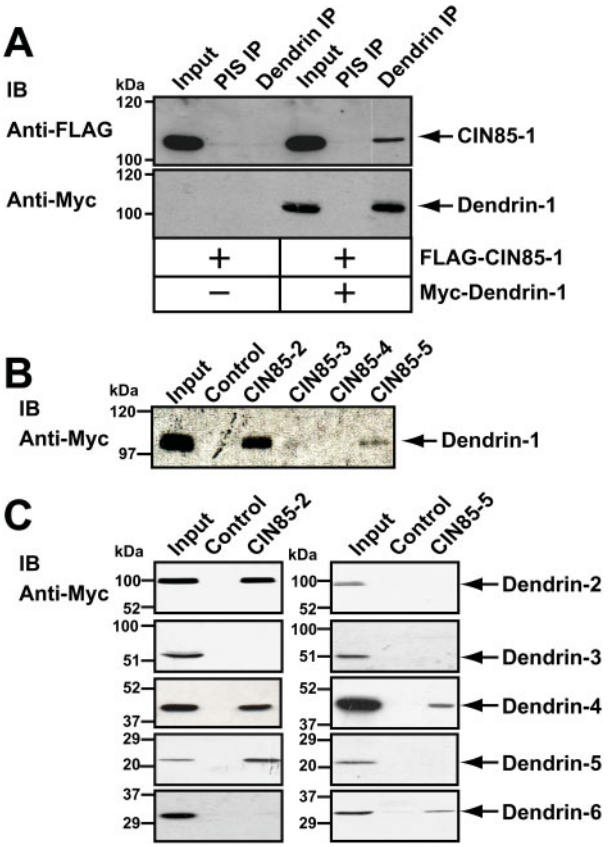

Fig. 5. **Interaction between dendrin and CIN85.** (A) Co-immunoprecipitation of dendrin and CIN85 in heterologous cells. FLAG-CIN85-1 was expressed alone or with Myc-dendrin-1 in COS-7 cells. Anti-dendrin antibody co-precipitated FLAG-CIN85-1 with Myc-dendrin-1. Input, cell lysates; PIS IP, immunoprecipitates with the preimmune serum; and Dendrin IP; immunoprecipitates with anti-dendrin serum. Protein standards are indicated on the left. (B) Mapping of dendrin-interacting region of CIN85. Pull-down assays were performed using lysates of COS-7 cells expressing Myc-dendrin-1 with various GST-CIN85 proteins immobilized on glutathione-Sepharose beads. The resulting complexes were analyzed by immunoblotting with anti-Myc antibody. GST-CIN85-2 efficiently trapped Myc-dendrin-1. GST-CIN85-5 also bound Myc-dendrin-1. (C) Mapping of CIN85-interacting region of dendrin. Pull-down assays were performed using lysates of COS-7 cells expressing various Myc-tagged dendrin proteins with GST-CIN85-2 and -5 immobilized on glutathione-Sepharose beads. GST-CIN85-2 interacted with Myc-dendrin-2, -4 and -5, while GST-CIN85-5 bound Myc-dendrin-4 and -6.

the interaction between CIN85 and dendrin, we expressed FLAG-CIN85 alone or with Myc-dendrin-1 in COS-7 cells and performed the immunoprecipitation by anti-dendrin antibody. FLAG-CIN85–1 was not immunoprecipitated by anti-dendrin antibody when expressed alone but co-immunoprecipitated with Myc-dendrin-1 (Fig. 5A). Next, we determined the dendrin-interacting region of CIN85. GST-CIN85-2 with the first SH3 domain efficiently trapped Myc-dendrin-1 (Fig. 5B). GST-CIN85-5 covering the C-terminal region also captured Myc-dendrin-1, but GST-CIN85-3 with the second SH3 domain or GST-CIN85-4 with the third SH3 domain did not. In the next set of experiments, we determined CIN85-interacting regions of dendrin. GST-CIN85-2 bound to Myc-dendrin-5 but not Myc-dendrin-6, while GST-CIN85-5 interacted with Myc-dendrin-6 but not Myc-dendrin-5 (Fig. 5C). Recent detailed studies have revealed that SH3 domains of CIN85 bind to an unusual binding motif PX(P/A)XXR (*39*). Because dendrin has PRPEPR immediately after the coiled-coil domain, we consider that this sequence may be responsible for the interaction with the first SH3 domain of CIN85. GST-CIN85-5 interacted with Myc-dendrin-4 and Myc-dendrin-6, but not with other constructs, suggesting that it binds not to the proline-rich region but to the extreme N-terminal region of dendrin (Fig 5C, right panel). As described above, the clone of CIN85 obtained in the yeast two-hybrid assay lacked the first N-terminal SH3 domain but, even so, interacted with dendrin bait. Taking these findings together, we concluded that dendrin and CIN85 interact with each other *via* multiple domains like the interaction between CIN85 and p85 subunit of phosphatidylinositol-3 (PI3)-kinase (*40*).

The N-Terminal Region of Dendrin Determines Its Nuclear Localization and CIN85 Induces the Partial Translocation of Dendrin—During this study, we noticed that the full-length Myc-dendrin is accumulated in the nucleus in COS-7 cells, while the N-terminal deleted Myc-dendrin is distributed in the cytosol (data not shown). As the immunocytostaining by anti-Myc antibody tends to exhibit a background signal in the nucleus, we confirmed the subcellular localization of various dendrin proteins with FLAG-tag (Fig. 6A). Dendrin has a putative nuclear localizing signal RKRR in the coiled-coil domain. As expected, proteins containing this sequence

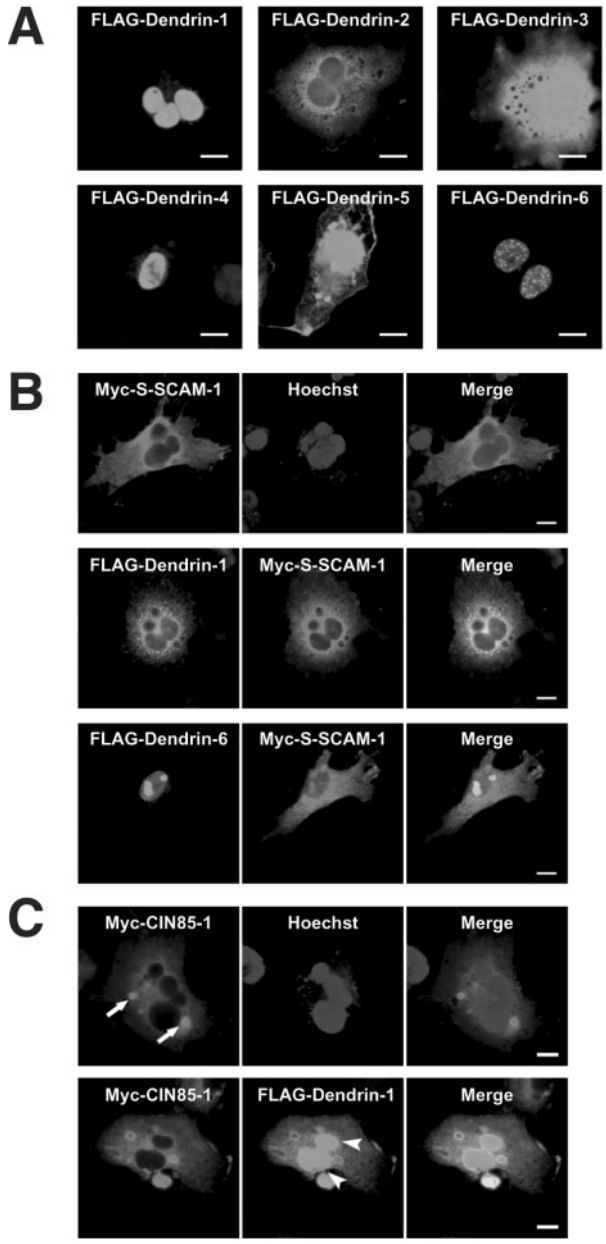

Fig. 6. **Effect of S-SCAM and CIN85 on the subcellular localization of dendrin.** (A) Nuclear localization of dendrin. Various FLAG-tagged dendrin proteins were expressed in COS-7 cells. Dendrin-1, -4 and -6 were mainly detected in the nucleus. Bars, 20 μm. (B) Effect of S-SCAM on the localization of dendrin. COS-7 cells were transfected with pClneoMyc S-SCAM-1 alone (top panel), pClneoMyc S-SCAM-1/pClneoFLAG dendrin-1 (middle panel) or pClneoMyc S-SCAM-1/pClneoFLAG dendrin-6 (bottom panel). Cells were fixed at 37°C and immunostained with mouse anti-Myc and rabbit anti-FLAG antibodies. Nuclei were visualized with Hoechst 33342. Myc-S-SCAM-1 was distributed in the cytosol (top panel). FLAG-dendrin-1 was recruited by Myc-S-SCAM-1 to the cytosol (middle panel). FLAG-dendrin-6 remained in the nucleus (bottom panel). Bars, 20 μm. (C) Effect of CIN85 on the localization of dendrin. COS-7 cells were transfected with pClneoMyc CIN85-1 alone (upper panel) or pClneoMyc CIN85-1/pClneoFLAG dendrin-1 (lower panel). Vesicle-like structures were detected (upper panel, arrows). FLAG-dendrin-1 partially shifted to the cytosol when co-expressed with Myc-CIN85-1, but signals still remained in the nucleus (lower panel, arrowheads). Bars, 20 μm.

(FLAG-dendrin-1, -4 and -6) were localized in the nucleus. S-SCAM showed a cytosolic distribution (Fig. 6B, top panel). FLAG-dendrin-1 was translocated to the cytosol when co-expressed with Myc-S-SCAM (Fig. 6B, middle panel). FLAG-dendrin-6 without the S-SCAM–interacting region remained in the nucleus (Fig. 6B, bottom panel). This result also supports the idea that S-SCAM interacts with the proline-rich region of dendrin. We next tested whether CIN85 had a similar effect on the localization of dendrin. Like S-SCAM, CIN85 was localized in the cytosol when expressed alone (Fig. 6C, upper panel). It is notable that vesicle-like structures were detectable (arrows). FLAG-dendrin-1 was partially detected in the cytosol when co-expressed with CIN85 (Fig. 6C, lower panel). However, dendrin was still partially detected in the nucleus (arrowheads). This result implies that CIN85 is less potent than S-SCAM in recruiting dendrin to the cytosol.

S-SCAM, CIN85 and Dendrin Form a Tripartite Complex In Vitro—We have not precisely mapped which sequences of dendrin are necessary for the interaction with S-SCAM and CIN85. As discussed above, however, the WW domains of S-SCAM and the SH3 domain of CIN85 are considered to recognize different motifs. Thereby, we speculated that S-SCAM and CIN85 can bind to dendrin simultaneously. We expressed in COS-7 cells Myc-S-SCAM-3 covering the WW domains and performed a pull-down assay with GST-CIN85-2. Myc-S-SCAM-3 was not captured by GST-CIN85-2 when expressed alone, but was trapped in the presence of Myc-dendrin-2 (Fig. 7A). This result indicates that the interactions of dendrin with the WW domains of S-SCAM and with the first SH3 domain of CIN85 are compatible with each other, even though both interacting sequences are closely located. Moreover, because the N-terminal region of dendrin interacts with the C-terminal region of CIN85, three proteins are more likely to form a complex. The immunofluorescence experiments using heterologous cells also support the formation of the tripartite complex. As shown above, the immunostaining of CIN85 in COS-7 cells at 37°C exhibited vesicle-like structures, and dendrin was detected around these structures with CIN85. The translocation of dendrin to the cytosol under this condition was incomplete and the recruitment of dendrin to the vesicle-like structures was not remarkable (Fig. 6C, lower panel). S-SCAM was not accumulated around these structures when co-expressed with CIN85 (Fig. 7B, upper panel). However, in the presence of dendrin and CIN85, S-SCAM also came to be detected on these structures (Fig. 7B, lower panel, arrowheads). Moreover, S-SCAM reciprocally enhanced the accumulation of dendrin to these structures (Fig. 7B, lower panel, arrows). The co-expression of GFP-dendrin and Myc-S-SCAM caused some accumulation of Myc-S-SCAM in the nucleus, while the co-expression of FLAG-dendrin and Myc-S-SCAM did not (Figs. 6B and 7B). We speculate that GFP-dendrin may be resistant to the nuclear export compared with FLAG-dendrin and reversely tether S-SCAM from the cytosol into the nucleus. In the last set of experiments, we attempted to determine the identity of these vesicle-like structures. We immunostained COS-7 cells expressing FLAG-CIN85-1 with anti-EEA1 and anti-Lamp1 antibodies. However, no co-localization was detected on these vesicles (data not shown). We also

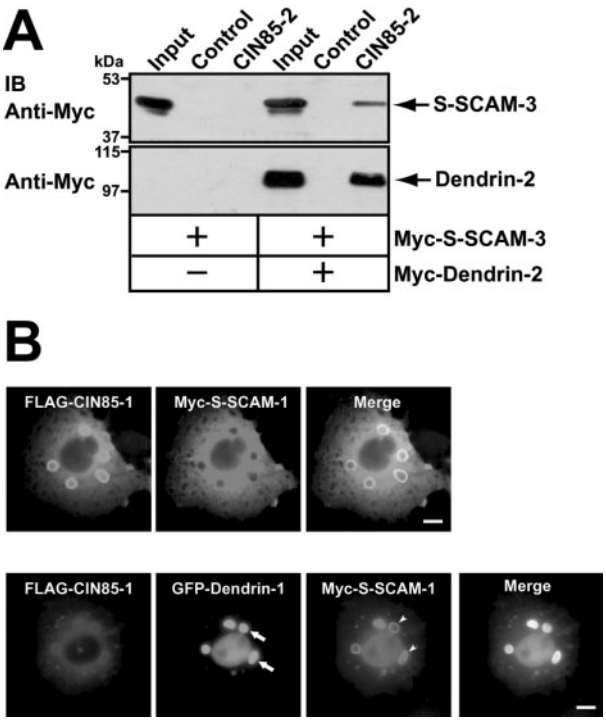

Fig. 7. **Dendrin forms a complex with S-SCAM and CIN85.** (A) Pull-down assays were performed using lysates of COS-7 cells expressing Myc-S-SCAM-3 alone or both Myc-S-SCAM-3 and Myc-dendrin-2 with GST-CIN85-2 immobilized on glutathione-Sepharose beads. GST-CIN85-2 did not directly trap Myc-S-SCAM-3 but captured it with Myc-dendrin-2. Protein standards are indicated on the left. (B) Co-localization of dendrin, S-SCAM and CIN85 in COS-7 cells. COS-7 cells were transfected with pClneoFLAG CIN85-1/pClneoMyc S-SCAM-1 (upper panel) or pBudCE- FLAG-CIN85-1-GFP-dendrin/pClneoMyc S-SCAM-1 (lower panel). Cells were fixed at 37°C and immunostained with mouse anti-Myc and rabbit anti-FLAG antibodies. FLAG-CIN85-1 was detected in the cytosol but the not accumulated to these structures. When GFP-dendrin-1 was co-expressed, Myc-S-SCAM-1 came to be accumulated to the vesicle-like structures (arrowheads). Dendrin was more remarkably concentrated than in Fig. 6C (arrows). Bars, 20 μm.

performed an incorporation assay using tetramethylrhodamine-conjugated EGF, but could find no accumulation of EGF in these structures (data not shown).

DISCUSSION

In this study, we demonstrated two novel protein–protein interactions, S-SCAM-dendrin and dendrin-CIN85. All three proteins are localized at dendritic spines in neurons and *in vitro* experiments using recombinant proteins support the interactions. S-SCAM and dendrin were co-immunoprecipitated from brain lysates. We also attempted to co-immunoprecipitate endogenous dendrin and CIN85 from brain (data not shown). However, dendrin is resistant to detergent extraction. We could recover only a small amount of endogenous dendrin in the detergent-soluble fraction, even with an ionic detergent such as deoxycholic acid. Also, because of the low sensitivity of the anti-dendrin antibody, we could not show the co-immunoprecipitation of endogenous dendrin and CIN85. In COS-7 cells, S-SCAM strongly recruited dendrin from the nucleus to the cytosol, as shown in Fig. 6, while CIN85 caused a partial translocation of dendrin. These observations suggest that the interaction between CIN85 and dendrin is looser than that between S-SCAM and dendrin. Pull-down assays indicated that dendrin binds to the WW domains of S-SCAM by the proline-rich region. Three sequences in this region fit with the WW domain–binding consensus motif. We have not determined which sequence is recognized by the WW domains of S-SCAM, but all of them may contribute to the interaction. Dendrin similarly binds to the WW domains of MAGI-1 *in vitro*. In the initial yeast two-hybrid screening, we used the C-terminal region of MAGI-1 as a bait and obtained the C-terminal region of dendrin as a prey. As yeast two-hybrid screening can detect protein–protein interactions with higher sensitivity, the results from pull-down assays in the presence of detergents do not completely exclude the possibility that dendrin interacts with MAGI-1 and putatively S-SCAM through the C-terminal region besides the WW domains. The interaction between S-SCAM and dendrin may take place in a manifold manner. We confirmed that dendrin binds to CIN85 at more than one site. The proline-rich region binds to the first SH3 domain of CIN85, while the N-terminal region of dendrin interacts with the C-terminal region of CIN85. It is known that CIN85 and p85 subunit of PI3-kinase interact with each other using multiple domains (*39*, *40*). CIN85 may generally use multiple interaction interfaces for its binding partner, so that it can simultaneously interact with more than one protein and form a large complex. *In vitro* biochemical experiments support the formation of a tripartite complex among S-SCAM, dendrin and CIN85. Although we have not confirmed the tripartite complex in neurons, co-expression experiments using heterologous cells suggest that these molecules indeed form a complex *in vivo*.

The physiological meanings of these interactions remain to be elucidated. In this study, we first encountered dendrin through the yeast two-hybrid screening of a kidney cDNA library. Dendrin has been studied as a brain protein, but we found that dendrin is expressed in non-neuronal tissues. MAGI-1 and MAGI-3, non-neuronal isoforms of S-SCAM, are widely expressed in various tissues. CIN85 and its closely related isoform named CD2AP are ubiquitously expressed in adult and fetal tissues (*33*). The interaction among dendrin, MAGI family protein and CIN85/CD2AP may be conserved in various tissues. During this study, Kremerskothen *et al.* independently reported the interaction between S-SCAM and dendrin (*41*). They noticed the S-SCAM–dependent recruitment of dendrin from the nucleus to the cytosol. They also analyzed how the message of dendrin is targeted to dendrites in neurons. Based on these findings, they have proposed that the message of dendrin is targeted to dendrites by its dendritic targeting element in the 3′ untranslated region and that S-SCAM retains the translated product at dendrites and prevents the nuclear transport. Despite this new report, it is largely unknown which role dendrin plays at dendrites. Our finding that dendrin links S-SCAM and CIN85 may hint about a putative role of dendrin. Overexpression experiments and the characterization of its binding partners support the notion that CIN85 is a versatile protein involved in different cellular functions. First, CIN85 is

involved in endocytosis and degradation of activated receptors including EGF receptor, Met and IgE receptor (*42*–*44*). Second, CIN85 is shown to activate p38 MAP kinase and is implicated in cellular stress response (*45*). Third, CIN85 negatively regulates PI3-kinase and interacts with apoptosis-linked gene 2–interacting protein (*37*, *38*). Its overexpression causes neuronal apoptosis and enhances tumor necrosis factor α-mediated apoptosis (*38*, *46*). S-SCAM directly interacts with NMDA receptor subunits and cell adhesion molecules and is involved in the accumulation of these proteins at synapses (*18*, *47*). The experiments using heterologous cells suggest that dendrin links S-SCAM to CIN85 and accumulates it to the vesicle-like structures. Endogenous CIN85 in COS-7 cells were detected at similar vesicle-like structures at 37°C (data not shown). Thereby, we speculate that these structures are not artifacts due to the overexpression of CIN85. Although we could not conclude that these structures are related to the endocytic process, the complex composed of S-SCAM, dendrin and CIN85 may be implicated in endocytosis of synaptic membrane proteins. This is an intriguing issue for future studies.

This study was supported by grants-in-aids for Scientific Research and on Priority Areas, and Special Coordination Funds for Promoting Science and Technology from the Ministry of Education, Culture, Sports, Science, and Technology, Yasuda Medical Research Foundation, and the Kao Foundation for Arts and Sciences. A.K., M.I., K.S. and A.K. are supported by Tokyo Medical and Dental University 21st century COE program "brain integration and its disorders".

REFERENCES

1. Dobrosotskaya, I., Guy, R.K., and James, G.L. (1997) MAGI-1, a membrane-associated guanylate kinase with a unique arrangement of protein-protein interaction domains. *J. Biol. Chem.* **275**, 21477–21485
2. Ide, N., Hata, Y., Nishioka, H., Hirao, K., Yao, I., Deguchi, M., Mizoguchi, A., Nishimori, H., Tokino, T., Nakamura, Y., and Takai, Y. (1999) Localization of membrane-associated guanylate kinase (MAGI)-1/BAI-associated protein (BAP) 1 at tight junctions of epithelial cells. *Oncogene* **18**, 7810–7815
3. Hirabayashi, S., Mori, H., Kansaku, A., Kurihara, H., Sakai, T., Shimizu, F., Kawachi, H. and Hata, Y. (2005) MAGI-1 is a component of the glomerular slit diaphragm that is tightly associated with nephrin. *Lab. Invest.* **85**, 1528–1543
4. Hirabayashi S., Tajima M., Yao I., Nishimura W., Mori H. and Hata Y. (2003) JAM4, a junctional cell adhesion molecule interacting with a tight junction protein, MAGI-1. *Mol. Cell. Biol.* **23**, 4267–4282
5. Patrie, K.M., Drescher, A.J., Goyal, M., Wiggins, R.C., and Margolis, B. (2001) The membrane-associated guanylate kinase protein MAGI-1 binds megalin and is present in glomerular podocytes. *J. Am. Soc. Nephrol.* **12**, 667–677
6. Wegmann, F., Ebnet, K., Du Pasquier, L., Vestweber, D., and Butz, S. (2004) Endothelial adhesion molecule ESAM binds directly to the multidomain adaptor MAGI-1 and recruits it to cell contacts. *Exp. Cell Res.* **300**, 121–133
7. Strochlic, L., Cartaud, A., Labas, V., Hoch, W., Rossier, J., and Cartaud, J. (2001) MAGI-1c: a synaptic MAGUK interacting with muSK at the vertebrate neuromuscular junction. *J. Cell Biol.* **153**, 1127–1132
8. Patrie, K.M., Drescher, A.J., Welihinda, A., Mundel, P., and Margolis, B. (2002) Interaction of two acting-binding proteins, synaptopodin and alpha-actinin-4, with the tight junction protein, MAGI-1. *J. Biol. Chem.* **277**, 30183–30190
9. Ohno, H., Hirabayashi, S., Kansaku, A., Yao, I., Tajima, M., Nishimura, W., Ohnishi, H., Mashima, Fujita, T, Omata, M., and Hata, Y. (2003) Carom: a novel membrane-associated guanylate kinase-interacting protein with two SH3 domains. *Oncogene* **22**, 8422–8431
10. Dobrosotskaya, I.Y. and James, G.L. (2000) MAGI-1 interacts with beta-catenin and is associated with cell-cell adhesion structures. *Biochem. Biophys. Res. Commun.* **270**, 903–909
11. Mino, A., Ohtsuka, T., Inoue, E., and Takai, Y. (2000) Membrane-associated guanylate kinase with inverted orientation (MAGI)-1/brain angiogenesis inhibitor I-associated protein (BAP1) as a scaffolding molecule for Rap small G protein GDP/GTP exchange protein at tight junctions. *Genes Cells* **5**, 1009–1016
12. Dobrosotskaya, I.Y. (2001) Identification of mNET1 as a candidate ligand for the first PDZ domain of MAGI-1. *Biochem. Biophys. Res. Commun.* **283**, 969–975
13. Sakurai, A., Fukuhara, S., Yamaguchi, A., Sato, K., Kamioka, Y., Masuda, M., Nakaoka, Y., and Mochizuki, N. (2006) MAGI-1 is required for Rap1 activation upon cell-cell contact and for enhancement of vascular endothelial cadherin-mediated cell adhesion. *Mol. Biol. Cell.* **17**, 966–976
14. Yao, R., Natsume, Y., and Noda, T. (2004) MAGI-3 is involved in the regulation of the JNK signaling pathway as a scaffold protein for frizzled and Ltap. *Oncogene* **23**, 6023–6030
15. Wu, Y., Dowbenko, D., Spencer, S., Laura, R., Lee, J., Gu, Q., and Lasky, L.A. (2000) Interaction of the tumor suppressor PTEN/MMAC with a PDZ domain of MAGI3, a novel membrane-associated guanylate kinase. *J. Biol. Chem.* **275**, 21477–21485
16. Adamsky, K., Arnold, K., Sabanay, H., and Peles, E. (2003) Junctional protein MAGI-3 interacts with receptor tyrosine phosphatase beta (RPTP beta) and tyrosine-phosphorylated proteins. *J. Cell Sci.* **116**, 1279–1289
17. Franklin, J.F., Yoshiura, K., Dempsey, P.J., Bogatcheval, G., Jeyakumra, L., Meise, K.S., Pearsall, R.S., Threadgill, D., and Coffey, R.J. (2005) Identification of MAGI-3 as a transforming growth factor-α tail binding protein. *Exp. Cell Res.* **303**, 457–470
18. Hirao, K., Hata, Y., Ide, N., Takeuchi, M., Irie, M., Yao, I., Deguchi, M., Toyoda, A., Sudhof, T.C., and Takai, Y. (1998) A novel multiple PDZ domain-containing molecule interacting with N-methyl-D-aspartate receptors and neuronal cell adhesion molecules. *J. Biol. Chem.* **273**, 21105–21110
19. Yap, C.C., Muto, Y., Kishida, H., Hashikawa, T., and Yano, R. (2003) PKC regulates the delta2 glutamate receptor interaction with S-SCAM/MAGI-2 protein. *Biochem. Biophys. Res. Commun.* **301**, 1122–1128.
20. Shoji, H., Tsuchida, K., Kishi, H., Yamakawa, N., Matsuzaki, T., Liu, Z., Nakamura, T., and Sugino, H. (2000) Identification and characterization of a PDZ protein that interacts with activin type II receptors. *J. Biol. Chem.* **275**, 5485–5492
21. Xu, J., Paquet, M., Lau, A.G., Wood, J.D., Ross, C.A., and Hall, R.A. (2001) Beta 1-adrenergic receptor association with the synaptic scaffolding protein membrane-associated guanylate kinase inverted-2 (MAGI-2). Differential regulation of receptor internalization by MAGI-2 and PSD-95. *J. Biol. Chem.* **276**, 41310–41317
22. Shi, S.H., Cheng, T., Jan, L.Y., and Jan, Y.N. (2004) The immunoglobulin family member dendrite arborization and synapse maturation 1 (Dasm1) controls excitatory synapse maturation. *Proc. Natl. Acad. Sci. USA* **101**, 13346–13351
23. Nishimura, W., Yao, I., Iida, J., Tanaka, N., and Hata, Y. (2002) Interaction of synaptic scaffolding molecule and beta-catenin. *J. Neurosci.* **22**, 757–765
24. Ide, N., Hata, Y., Deguchi, M., Hirao, K., Yao, I., and Takai, Y. (1999) Interaction of S-SCAM with neural plakophilin-related

Armadillo-repeat protein/delta-catenin. *Biochem. Biophys. Res. Commun.* **256**, 456–461
25. Wu, X., Hepner, K., Castelino-Prabhu, S., Do, D., Kaye, M.B., Yuan, X.J., Wood, J., Ross, C., Sawyers, C.L., and Whang, Y.E. (2000) Evidence for regulation of the PTEN tumor suppressor by a membrane-localized multi-PDZ domain containing scaffold protein MAGI-2. *Proc. Natl. Acad. Sci. USA* **97**, 4233–4238
26. Ohtsuka, T., Hata, Y., Ide, N., Yasuda, T., Inoue, E., Inoue, T., Mizoguchi, A., and Takai, Y. (1999) nRap GEP: a novel neural GDP/GTP exchange protein for rap1 small G protein that interacts with synaptic scaffolding molecule (S-SCAM). *Biochem. Biophys. Res. Commun.* **265**, 38–44
27. Wood, J.D., Yuan, J., Margolis, R.L., Colomer, V., Duan, K., Kushi, J., Kaminsky, Z., Kleiderlein, J.J., Sharp, A.H., and Ross, C.A. (1998) Atrophin-1, the DRPLA gene product, interacts with two families of WW domain-containing proteins. *Mol. Cell. Neurosci.* **11**, 149–160
28. Hirao, K., Hata, Y., Yao, I., Deguchi, M., Kawabe, H., Mizoguchi, A., and Takai, Y. (2000) Three isoforms of synaptic scaffolding molecule and their characterization. Multimerization between the isoforms and their interaction with N-methyl-D-aspartate receptors and SAP90/PSD-95-associated protein. *J. Biol. Chem.* **275**, 2966–2972
29. Hirabayashi, S., Nishimura, W., Iida, J., Kansaku, A., Kishida, S., Kikuchi, A., Tanaka, N., and Hata, Y. (2004) Synaptic scaffolding molecule interacts with axin. *J. Neurochem.* **90**, 332–339
30. Yao, I., Hata, Y., Ide, N., Hirao, K., Deguchi, M., Nishioka, H., Mizoguchi, A., and Takai, Y. (1999) MAGUIN, a novel neuronal membrane-associated guanylate kinase-interacting protein. *J. Biol. Chem.* **274**, 11889–11896
31. Neuner-Jehle, M., Denizot, J.P., Borbely, A.A., and Mallet, J. (1996) Characterization and sleep deprivation-induced expression modulation of dendrin, a novel dendritic protein in rat brain neurons. *J. Neurosci. Res.* **46**, 138–151
32. Herb, A., Wisden, W., Catania, M.V., Marechal, D., Dresse, A., and Seeburg, P.H. (1997) Prominent dendritic localization in forebrain neurons of a novel mRNA and its product, dendrin. *Mol. Cell. Neurosci.* **8**, 367–374
33. Dikic, I. (2002) CIN85/CMS family of adaptor molecules. *FEBS Lett.* **529**, 110–115
34. Kansaku, A., Hirabayashi, S., Mori, H., Fujiwara, N., Kawata, A., Ikeda, M., Rokukawa, C., Kurihara, H., and Hata, Y. Ligand-of-Numb protein X is an endocytic scaffold for junctional adhesion molecule 4. *Oncogene* in press.
35. Sudol, M., Sliwa, K., and Russo, T. (2001) Functions of WW domains in the nucleus. *FEBS Lett.* **490**, 190–195
36. Take, H., Watanabe, S., Takeda, K., Yu, Z.X., Iwata, N., and Kajigaya, S. (2000) Cloning and characterization of a novel adaptor protein, CIN85, that interacts with c-Cbl. *Biochem. Biophys. Res. Commun.* **268**, 321–328
37. Gout, I., Middleton, G., Adu, J., Ninkina, N.N., Drobot, L.B., Filonenko, V., Matsuka, G., Davies, A.M., Waterfield, M., and Buchman, V.L. (2000) Negative regulation of PI 3-kinase by Ruk, a novel adaptor protein. *EMBO J.* **19**, 4015–4025
38. Chen, B., Borinstein, S.C., Gillis, J., Sykes, V.W., and Bogler, O. (2000) The glioma-associated protein SETA interacts with AIP1/Alix and ALG-2 and modulates apoptosis in astrocytes. *J. Biol. Chem.* **275**, 19275–19281
39. Kurakin, A.V., Wu, S., and Bredesen, D.E. (2003) Atypical recognition consensus of CIN85/SETA/Ruk SH3 domains revealed by target-assisted iterative screening. *J. Biol. Chem.* **278**, 34102–34109
40. Borthwick, E.B., Korobko, I.V., Luke, C., Drel, V.R., Fedyshyn, Y.Y., Ninkina, N., Drobot, L.B., and Buchman, V.L. (2004) Multiple domains of Ruk/CIN85/SETA/CD2BP3 are involved in interaction with p85alpha regulatory subunit of PI 3-kinase. *J. Mol. Biol.* **343**, 1135–1146
41. Kremerskothen, J., Kindler, S., Finger, I., Veltel, S., and Barnekow, A. (2006) Postsynaptic recruitment of dendrin depends on both dendritic mRNA transport and synaptic anchoring. *J. Neurochem.* **96**, 1659–1666
42. Soubeyran, P., Kowanetz, K., Szymkiewicz, I., Lngton, W.Y., and Dikic, I. (2002) Cbl-CIN85-endophilin complex mediates ligand-induced down-regulation of EGF receptors. *Nature* **416**, 183–187
43. Petrelli, A., Gilestro, G.F., Lanzardo, S., Comoglio, P.M., Migone, N., and Giordano, S. (2002) The endophilin-CIN85-Cbl complex mediates ligand-dependent down-regulation of c-Met. *Nature* **416**, 187–190
44. Molfetta, R., Belleudi, F., Peruzzi, G., Morrone, S., Leone, L., Dikic, I., Piccoli, M., Frati, L., Torrisi, M.R., Santoni, A., and Paolini, R. (2005) CIN85 regulates the ligand-dependent endocytosis of the IgE receptor: a new molecular mechanism to dampen mast cell function. *J. Immunol.* **175**, 4208–4216
45. Aissouni,Y., Zapart, G., Iovanna,J.L., Dikic, I., and Soubeyran, P. (2005) CIN85 regulates the ability of MEKK4 to activate the p38 MAP kinase pathway. *Biochem. Biophys. Res. Commun.* **338**, 808–814
46. Narita, T., Nishiumra, T., Yoshizaki, K., and Taniyama, T. (2005) CIN85 associates with TNF receptor 1 via Src and modulates TNF-α-induced apoptosis. *Exp. Cell Res.* **304**, 256–264
47. Iida, J., Hirabayashi, S., Sato, Y., and Hata, Y. (2004) Synaptic scaffolding molecule is involved in the synaptic clustering of neuroligin. *Mol. Cell. Neurosci.* **27**, 497–508